

# Design and analysis of an origami-based three-finger manipulator

Donghwa Jeong and Kiju Lee\*

*Department of Mechanical and Aerospace Engineering, Case Western Reserve University, Cleveland, 44106 Ohio, USA. E-mail: donghwa.jeong@case.edu*

(Accepted July 28, 2017. First published online: September 7, 2017)

## SUMMARY

This paper describes a new robotic manipulator with three fingers based on an origami twisted tower design. The design specifications, kinematic description, and results from the stiffness and durability tests for the selected origami design are presented. The robotic arm is made of a 10-layer twisted tower, actuated by four cables with pulleys driven by servo motors. Each finger is made of a smaller 11-layer tower and uses a single cable directly attached to a servo motor. The current hardware setup supports vision-based autonomous control and internet-based remote control in real time. For preliminary evaluation of the robot's object manipulation capabilities, arbitrary objects with varying weights, sizes, and shapes (i.e., a shuttlecock, an egg shell, a paper cub, and a cubic block) were selected and the rate of successful grasping and lifting for each object was measured. In addition, an experiment comparing a rigid gripper and the new origami-based manipulator revealed that the origami structure in the fingers absorbs the excessive force applied to the object through force distribution and structural deformation, demonstrating its potential applications for effective manipulation of fragile objects.

**KEYWORDS:** Origami robot; Robotic manipulator; Manipulator design; Manipulator kinematics.

## 1. Introduction

This paper presents a three-finger robotic manipulator based on an origami structure called *twisted tower*, which was first designed by Mihoko Tachibana. This particular origami design allows spring-like behaviors, suitable for generating linear contraction and extension as well as bending motions. In our previous work presented at IROS 2014,<sup>1</sup> the twisted tower was used to build a crawling robot and a robotic arm to physically demonstrate its potential applications in functional robot units. Building on our prior work, a robotic arm with three fingers was built and tested for object manipulation (Fig. 1). This robotic manipulator is called *OrigamiBot-II*. OrigamiBot-II is actuated by servo motors—four for the arm and three for the fingers. It is hung on a wooden frame and equipped with a camera at the gripper plate, on which the fingers are attached, facing downward.

### 1.1. Related work

Origami, the art of paper folding, has received considerable research interest in mathematics and art.<sup>2–5</sup> More recently, it has inspired engineers in various applications, such as a DNA folding mechanism, design of medical stents, design of crumple zones in automobiles, and architecture designs.<sup>3</sup> For example, origami has been used in structural applications for its coexisting properties of flexibility and rigidity that the folding patterns provide.<sup>6</sup> Origami structures were also found useful in shelter systems as well as in a novel vehicle crash box designed for absorbing energy during a collision.<sup>7,8</sup> In robotics, origami has demonstrated useful functionalities, such as actuators,<sup>9,10</sup> springs,<sup>11</sup> and printable robots.<sup>12</sup> Origami has also been adopted for deformable wheels in mobile robots. For example, reconfigurable origami wheels were used to facilitate fast movement with large wheels and access through small gaps by folding and reducing the wheel diameter.<sup>13</sup> A similar method was also

\* Corresponding author. E-mail: kiju.lee@case.edu



Fig. 1. OrigamiBot-II: Three-finger origami manipulator using the origami twisted tower for constructing the arm and fingers. Four servo motors, installed on the top of the frame, control the arm and three mini-servos control the three fingers for grasping an object.

adopted to achieve amphibious locomotion on both ground and water surfaces.<sup>14</sup> Due to the structural properties, actuation of such robotic systems often employs a cable-driven mechanism. In particular, many of the previous robotic designs inspired by origami utilized folding features actuated by Shape Memory Alloys (SMAs), mainly due to the light weight. The SMAs are used to extend and contract the structure when a specific amount of heat is applied by current.<sup>15</sup> Although there are SMAs that are activated at a low temperature ( $70^{\circ}\text{C}$ ), the origami must use materials that are thermally resistant, such as polyester, polyether (PEEK), or polytetrafluoroethylene (PTFE).<sup>12</sup>

Most of these existing origami robots have been aimed at achieving mobility, through leg-based walking and crawling or wheel-based locomotion. However, little attention has been paid toward the use of origami in object manipulation. Some of the origami designs, such as the twisted tower used in our work, have structural properties that are uniquely suited for a manipulator. Some other non-traditional approaches for robotic manipulation use soft materials in the gripper or arm, deviating from the exclusive use of rigid materials.<sup>16–20</sup> Due to the non-rigidity in the structure, actuation strategies for soft robots differ from those typically used in rigid robots. Common actuators, such as pneumatic/hydraulic actuators or motors, are often used in combination with a cable-driven mechanism. For example, an octopus-like robot uses cables with servo motors to actuate silicone arms.<sup>16</sup> SMAs may replace the cable-driven actuators while reducing the system complexity and size.<sup>17</sup> Another cable-driven mechanism resembles an elephant's trunk.<sup>18</sup> In this work, cables run through the backbone and segment plates in order to generate bending motions in the manipulator.<sup>18</sup> This study derived and numerically solved the non-linear kinematics for a single segment of a continuous backbone robot and provided the optimal distance between two segments for maximum displacement, load capacity, and simplicity of the robot kinematics. Another similar elephant-like robot has a trunk manipulator consisting of four small links (springs) between each layer and actuated by a cable-servo system.<sup>19</sup>

There are some soft robots that operate without using a cable-driven mechanism for actuation. For example, OctArm is contracted and extended by using pressurized air in its elastic tubes.<sup>20</sup> This robot successfully demonstrated the ability to grasp and manipulate objects over a wide range of sizes and weights. It was also tested in open air and water to show adaptive manipulating ability in a challenging environment. Another interesting robot, made of five layers of materials cut by a laser cutter, can fold when heated by using sandwiched layers of copper, papers, and shape-memory polymers.<sup>21</sup> Another soft manipulator that used reversible jamming of granular media was able to grasp irregular-shaped objects by tuning its stiffness.<sup>22</sup>

In this paper, a new origami-based robotic manipulator with three fingers is presented. The arm and each finger are made of origami twisted towers, which resembles a continuum robot arm where



Fig. 2. Twisted tower in different configurations showing linear extension and contraction and bending. Each layer can be configured to be folded in one of the two directions.

the arm is actuated by four cables and each finger is actuated by a single cable. The towers can generate different workspaces depending on the routing of the cables. The cables must be routed carefully in order to avoid possible buckling. While the current robot uses a specific routing method, potential alternatives are also discussed in this paper. To demonstrate the robot's object manipulation capabilities, grasping and lifting tests were performed using several objects with different geometries, textures, and weights.

The rest of the paper is organized as follows. Section 2 describes the selected origami design, kinematics, and results from the stiffness and durability tests. In Section 3, the hardware architecture and design of the robot are presented, including actuation strategy, embedded sensors and electronics, and workspace analysis. The robot's capabilities for manipulating arbitrary objects, such as a shuttlecock, egg shell, paper cup, and cube block, were tested; the results are provided in Section 4.

## 2. Origami Twisted Tower

### 2.1. Design considerations

A successful design for a robotic manipulator should meet the following criteria:

- **Reconfigurability** to generate motions.
- **Structural stability** to maintain certain ranges of shapes.
- **Load bearing** to manipulate objects.

After analysis of many origami designs, the twisted tower design by Mihoko Tachibana was selected.<sup>1,2</sup> This design was used to build a robotic arm with three fingers. The twisted tower is made of identical origami segments that are connected in an octagonal pattern and stacked to form a tower. To begin creating the tower, a single piece of rectangular paper is selected and folded following a specific sequence. The size of the rectangular piece determines the diameter and height of each octagon layer, and therefore must be determined based on the desired size of the arm and workspace.<sup>1</sup> The twisted tower requires 24 origami segments for the first octagon layer and 16 segments for each additional layer. Any number of octagon layers can be added to form a tower with a desired height. Figure 2 shows extending, contracting, and bending motions realized by the twisted tower. The relative orientations of the top and base layers are dependent upon the twisting direction in each layer. The twisted tower behaves like a spring, while the overall diameter remains the same during extension and contraction. In addition, the “modular” origami design, referring to an assembly of multiple origami segments, keeps it more stable and durable than single-paper origami patterns.<sup>11</sup>

### 2.2. Kinematics

*Nomenclature:*

- $h$ : The length of a side on the octagon.
- $l_i$ : The distance between the top and the bottom layer when only twisting (“screw” motion) is applied between the top and bottom plates.
- $\theta_i$ : The torsional angle between the bottom and top plates measured about  $\hat{z}_{i-1}$ .
- $\alpha_i$ : The rotation about  $\hat{z}_{i-1}$  for  $\hat{x}_{i-1}$  to point the bending direction.
- $\phi_i$ : The bending angle at the  $i$ th layer.
- $d_i$ : The distance between the centers of the two plates after bending is applied.

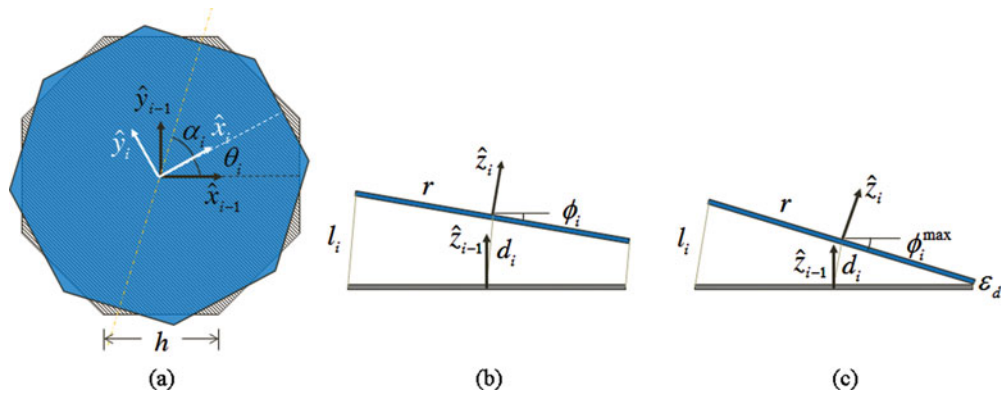


Fig. 3. (a) Top view of a single tower layer, (b) side view along where the bending occurs, and (c) side view along where the maximum bending (i.e.,  $\phi_i = \phi_i^{\max}$ ) occurs. The twisting angle between the top plate (blue) and the bottom plate (gray) is  $\theta_i$ . After twisting, bending motion is applied toward one of the eight sides, where  $0 \leq \alpha_i \leq 2\pi$  and  $\phi_i$  is the bending angle.  $d_i$  is the distance between the centers of the two frames.

The twisted tower structure shows low bending stiffness and high axial stiffness because papers bend easily but barely stretch. Therefore, the structure generates “rigid-body-like” motions that allow us to adopt conventional rigid-body kinematics with physical constraints associated with the paper thickness and structural limitations. It is assumed that the top and bottom plates of the octagon layer are rigid, so that possible motions between the two plates are limited to (1) linear displacement via twisting about the vertical axis while keeping the top and bottom plates parallel and (2) bending toward one of the eight outer edges of the octagon layer.

In our previous work,<sup>1</sup> the kinematics of the structure is derived individually for each twisting and bending motion within a single layer. In this paper, a transformation matrix from the bottom plate to the top plate for each layer is defined slightly differently as a screw motion combined with a bending motion, as shown in Fig. 3.  $\theta_i$  denotes the twist angle between the top and bottom plates, such that  $-\pi/4 + \epsilon_\theta \leq \theta_i \leq \pi/4 - \epsilon_\theta$  where  $\epsilon_\theta$  is a small angle caused by the thickness of the layer when fully collapsed. The octagon layer may generate pure screw motion while keeping the top and bottom plates parallel to each other and changing  $\theta_i$  only, resulting in linear displacement of

$$l_i \approx h - \frac{4h}{\pi} |\theta_i|. \tag{1}$$

Bending between the top and bottom plates may occur toward any direction, such that  $0 \leq \alpha_i < 2\pi$ . As shown in Figs. 3b and 3c, the bending angle is limited by  $0 \leq \phi_i \leq \phi_i^{\max}$ , where

$$\phi_i^{\max} = 2 \sin^{-1} \left( \frac{l_i - \epsilon_d}{4r} \right). \tag{2}$$

$\epsilon_d$  denotes a small displacement between the two plates caused by the thickness of the folded structure. Using Eq. (1), the relationship between  $\epsilon_\theta$  and  $\epsilon_d$  can be achieved by

$$\epsilon_d = h - \frac{4h}{\pi} \left( \frac{\pi}{4} - \epsilon_\theta \right).$$

The distance between two frames attached at the bottom and the top plates,  $d_i$ , can be then calculated by

$$d_i = l_i - 2r \sin \left( \frac{\phi_i}{2} \right). \tag{3}$$

The transformation from the frame attached at the bottom center to the frame at the top center of the octagon layer is determined by following the sequence listed below:

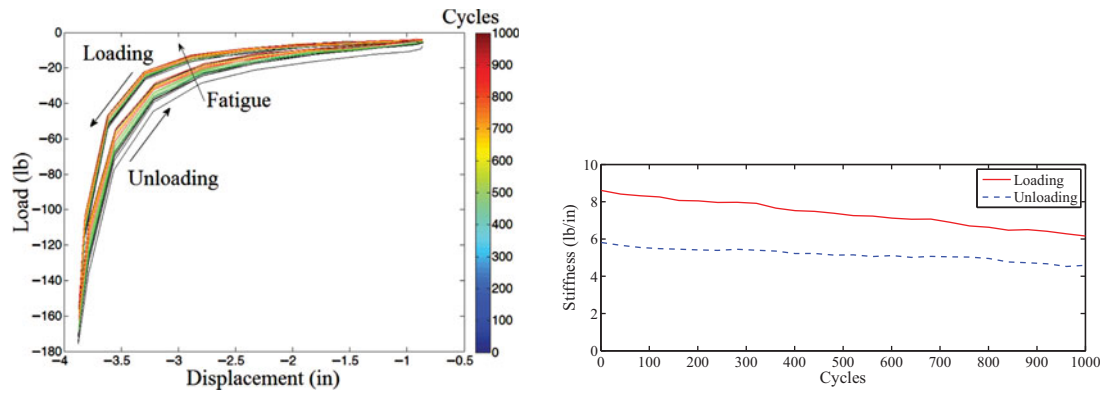


Fig. 4. Performance result of 1000 cycles of loading and unloading origami structure (left) and stiffness changes induced by fatigue (right). The color bar in the left graph shows the number of cycles of the loading and unloading up to 1000 cycles.<sup>1</sup>

- Assign a frame  $\{i - 1\}$  to the bottom center of the octagon layer and rotate it by  $\theta_i$  about  $\hat{z}_{i-1}$ .
- Rotate the frame again by  $\alpha_i$  about the  $z$ -axis to align the  $x$ -axis toward bending direction.
- Rotate  $\phi_i/2$ , half of the total bending angle, about the  $y$ -axis.
- Move the frame by  $d_i$  along the  $z$ -axis.
- Rotate  $\phi_i/2$  about the  $y$ -axis.
- Finally, reorient the frame by rotating  $-\alpha_i$  along  $\hat{z}_i$ .

The corresponding rigid-body transformation is calculated as follows:

$$T_i = R_z(\alpha_i) \cdot R_z(\theta_i) \cdot R_y(\phi_i/2) \cdot \text{Trans}_z(d_i) \cdot R_y(\phi_i/2) \cdot R_z(-\alpha_i)$$

$$= \begin{pmatrix} s\beta_i s\alpha_i + c\beta_i c\alpha_i c\phi_i & c\beta_i c\phi_i s\alpha_i - s\beta_i c\alpha_i & c\beta_i s\phi_i & d_i s\frac{\phi_i}{2} c\beta_i \\ s\beta_i c\alpha_i c\phi_i - c\beta_i s\alpha_i & c\beta_i c\alpha_i + s\beta_i c\phi_i s\alpha_i & s\beta_i s\phi_i & d_i s\frac{\phi_i}{2} s\beta_i \\ -c\alpha_i s\phi_i & -s\alpha_i s\phi_i & c\phi_i & d_i c\frac{\phi_i}{2} \\ 0 & 0 & 0 & 1 \end{pmatrix}, \quad (4)$$

where  $\beta_i = \theta_i + \alpha_i$  for shorthand writing. Note that  $R_x$ ,  $R_y$ , and  $R_z$  indicate rotations about the  $x$ -,  $y$ -, and  $z$ -axis, respectively, and  $\text{Trans}_z$  is pure translation along the  $z$ -axis. We also note that the order of the first two rotation matrices,  $R_z(\alpha_i)$  and  $R_z(\theta_i)$ , in Eq. (4) are switched intentionally to simplify the composite transformation matrix. For  $n$  layers, transformation from the bottom plate of the first layer to the top plate of the  $n$ th layer is given by

$$T = T_1 T_2 \cdots T_{n-1} T_n = \prod_{i=1}^n T_i.$$

### 2.3. Stiffness and durability<sup>1</sup>

To estimate the stiffness and force capacity as well as dynamic characteristics such as fatigue over time, a twisted tower made of construction paper was tested by an Instron servo-hydraulic testing machine (model 8501).<sup>1</sup> This machine has a maximum displacement of 4 inches, so a six-layer twisted tower with maximum 3-inch stroke was used for testing. A total of 1000 sinusoidal cycles were modeled with 1 Hz frequency and 1.5-inch amplitude (3-inch stroke). A 250 lb capacity force transducer was used for the test. As shown in Fig. 4 (left), the average stiffness for 1-inch contraction to 3-inch contraction was 8.61 pound/inch (lb/in) for loading and 5.81 lb/in for unloading at the first cycle. Another observation was the fatigue of the structure by repetitive motion. Figure 4 (right) shows that the stiffness changed gradually over time. It is anticipated that the stiffness and fatigue properties would vary depending on (1) the number of the layers, (2) physical size, and (3) material used to fold the structure.

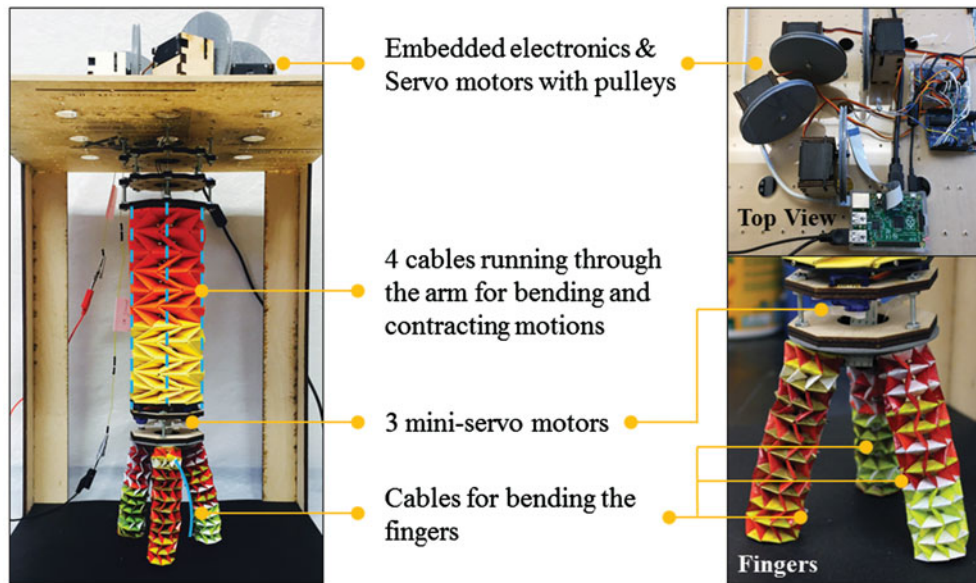


Fig. 5. OrigamiBot-II is upheld in a box frame. Four servo motors with pulleys and associated electronics for pulling and releasing the cables to control the arm are installed on the top of the box frame. Four cables linearly run through the arm's origami structure in a zig-zag pattern, enabling linear contraction and extension and bending. The gripper plate holds three mini-servo motors for the fingers.

### 3. Hardware Design

#### 3.1. Technical specifications

OrigamiBot-II consists of a manipulator arm with three fingers. The arm uses  $4.25(w) \times 2.125(h) \times 0.012(t)$  pieces of construction paper. In the folded twisted tower,  $h = 1.35$ ,  $r = 1.7639$ , and  $\epsilon_{\theta}^{\text{arm}} = 0.113$ . All lengths were measured in inches and angles in radians. For each finger,  $1.38 \times 0.78 \times 0.0015$  pieces of polyethylene film were used, resulting in  $h = 0.5$ ,  $r = 0.6533$ , and  $\epsilon_{\theta}^{\text{finger}} = 0.09$ . The polyethylene film was used for the fingers as an alternative to construction paper. Construction paper was too thick for folding such a small tower. The total length of the arm is 10 and each finger is 6 when fully extended. The maximum stroke of the arm is about 6. The arm is actuated by four cables (i.e., nylon wires) with four servo motors (Fig. 5). Each finger has a single cable directly connected to a mini-servo motor for generating bending motion. The cables in the arm were internally routed through holes in the twisted tower while the cable on the finger was externally routed (Fig. 6). The twisted towers used for the fingers were too small and the material was fragile to make holes, so metal hooks were attached to the outside of the structure.

OrigamiBot-II was supported by a  $16(w) \times 16(d) \times 18(h)$  box frame, where the associated controllers and circuits were installed on top of the box (Fig. 5). The arm and fingers were naturally released due to gravity, resulting in 9 and 4.65 in length, respectively. Only pulling force was applied to the cables in the fingers and arm. Three mini-servo motors were located on the gripper plate that holds three fingers. The maximum power consumption without payload at the gripper is about 10 W with the fully contracted arm and fingers and less than 2 W when released by gravity. The control board consists of two main processing units: Raspberry Pi and Arduino Uno R3. The Raspberry Pi used embedded graphical processing algorithms to process the captured video images while the Arduino controls the servo motors. Raspberry Pi B+, which adopts 700 MHz single-core ARM CPU and 250 MHz Broadcom VideoCore IV GPU, was used as the main video processing module. A 5-megapixel high-resolution camera was installed at the gripper plate to capture images at a high data rate during manipulation using a camera serial interface (CSI) to Raspberry Pi.

To actuate the arm, four SG-5010 motors were installed on the top of the manipulator. Each of these motors pulls (or releases) a nylon cable rolled on a 3D-printed pulley, providing 9.55 lbf-in. The radius of the pulley is 2 and the maximum force to pull the cable is 4.85 lbf. For the gripper, three SG-90 motors were installed on the gripper plate for bending each of the three fingers. The motor

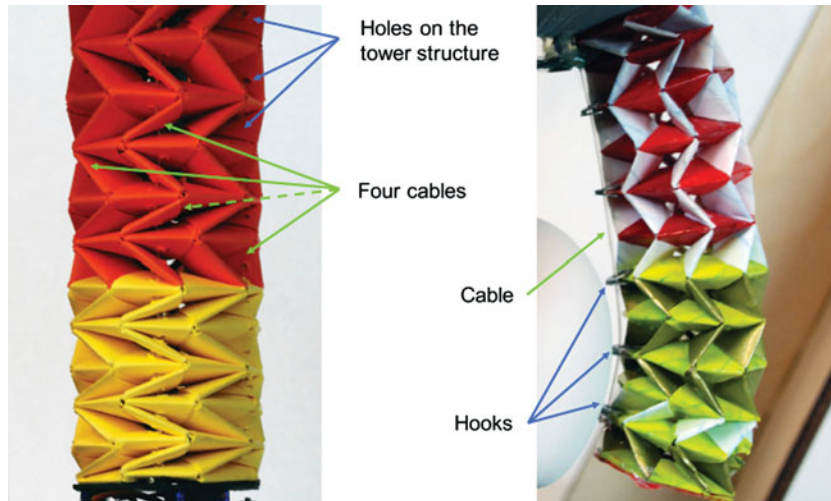


Fig. 6. Four cables are routed through holes on the tower structure in a zig-zag pattern for the arm and a single cable runs through hooks in each finger.

can pull the cable with 1.56 lbf-in. The cable is connected at a 1.18 inch distance from the servo axis so that each finger is bent by a 1.32 lb pulling force. Arduino Uno R3, used as the main processing board for motor control, provides an easy programming and debugging environment for sensor-based feedback control of the motors. Raspberry Pi requires an external Analog to Digital Converter (ADC), such as MCP3008 or ADS1115, for analog sensing and thus requires a logic converter to use 5 V processing modules. In addition, Arduino Uno R3 collects the analog data and performs the motor control by using the pre-installed library and built-in functions.

### 3.2. Workspace analysis

Workspace of the twisted tower is affected by the number of layers, the number of cables used for actuation, and how these cables are routed. Subsections of the tower may be independently actuated by individual cables, which may be routed in different patterns. In OrigamiBot-II, four cables were routed in a zig-zag pattern, generating linear and bending motions without a twist. Pulling and releasing the cables cannot cause buckling in this case. The kinematic workspace of OrigamiBot-II was estimated by the reachable positions of the end-effector, i.e., the center of the bottom plate of the suspended manipulator.

In OrigamiBot-II, every two layers collapse in alternating directions, such that  $\theta_1 = -\theta_2 = \theta_3 = \dots = -\theta_{10}$ , generating linear translation or bending without any torsional angle:

$$T_i T_{i+1} = R_z(\alpha) \begin{pmatrix} c(\phi_i + \phi_{i+1}) & 0 & s(\phi_i + \phi_{i+1}) & d_i s \frac{\phi_i}{2} + d_{i+1} s(\phi_i + \frac{\phi_{i+1}}{2}) \\ 0 & 1 & 0 & 0 \\ -s(\phi_i + \phi_{i+1}) & 0 & c(\phi_i + \phi_{i+1}) & d_i c \frac{\phi_i}{2} + d_{i+1} c(\phi_i + \frac{\phi_{i+1}}{2}) \\ 0 & 0 & 0 & 1 \end{pmatrix} R_z(-\alpha)$$

for all  $i = 1, 3, \dots, 9$ , where  $\alpha$  indicates the bending direction. Then the composite transformation for 10 layers is given by

$$T = \prod_{i=1}^{10} T_i = R_z(\alpha) \begin{pmatrix} c\Phi & 0 & s\Phi & D_x \\ 0 & 1 & 0 & 0 \\ -s\Phi & 0 & c\Phi & D_z \\ 0 & 0 & 0 & 1 \end{pmatrix} R_z(-\alpha), \tag{5}$$

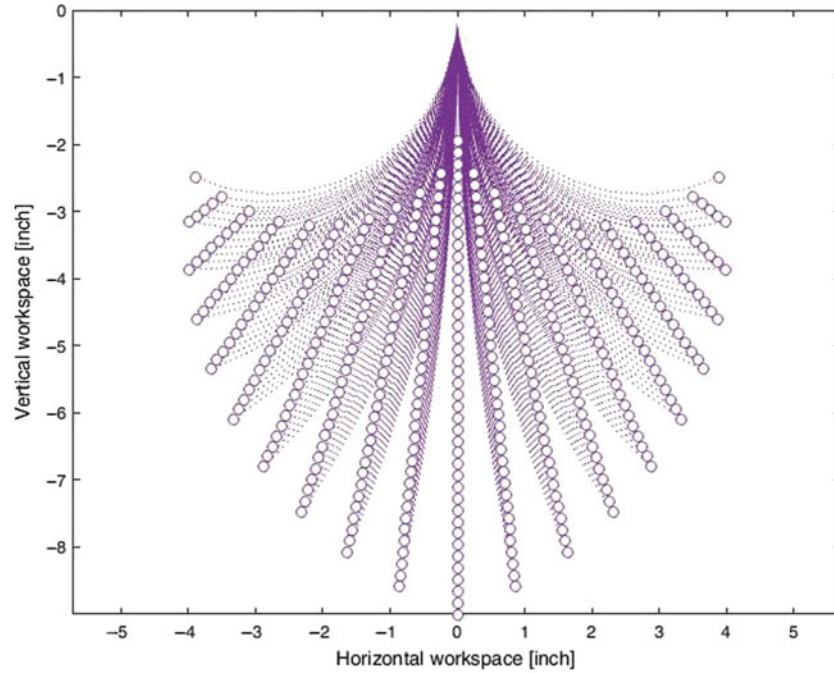


Fig. 7. Reachable workspace for the arm when  $\alpha = 0$  and  $\alpha = \pi$  based on the simplified kinematics and measured parameters. “o” indicates the end-effector positions. The workspace is defined by the area bounded by the outer boundaries.

where

$$\Phi = \sum_{k=1}^{10} \phi_k; \quad D_x = \sum_{k=1}^{10} d_k \sin\left(\sum_{j=1}^k \phi_j - \frac{\phi_k}{2}\right); \quad D_z = \sum_{k=1}^{10} d_k \cos\left(\sum_{j=1}^k \phi_j - \frac{\phi_k}{2}\right).$$

Further assuming that the cable-driven mechanism generates uniform transformation across the layers, the above terms are further simplified as

$$\Phi = 10\phi; \quad D_x = d \sum_{k=1}^{10} \sin((k - 0.5)\phi); \quad D_z = d \sum_{k=1}^{10} \cos((k - 0.5)\phi), \quad (6)$$

where  $\phi$  is the bending angle in every layer. In OrigamiBot-II,  $h = 1.35$  and  $\epsilon_\theta = 0.113$ . When the arm is naturally released, it cannot fully stretch out due to the pre-folded configuration, resulting in  $\theta_{\min} = 0.2618$ . Figure 7 shows the kinematic workspace of the arm using these parameters, where  $\alpha = 0$  and  $\alpha = \pi$ . While this shows reachable positions of the end-effector for the given geometrical properties, the actual workspace requires considering both theoretical assumption and physical parameters. The assumption of uniform bending across the tower is reasonable if the arm moves horizontally without significant gravity effect. However, the current hardware structure has the arm upheld by the frame. In particular, additional weight due to the gripper and a camera as well as an external object manipulated by the gripper has influence to the reachable workspace. We are currently working on modified workspace analysis taking the gravity effect into account.

## 4. Experiments

### 4.1. Control strategy

OrigamiBot-II supports real-time teleoperation through internet. The hardware configuration of the overall system consists of the manipulator and a remote computing device (e.g., a computer

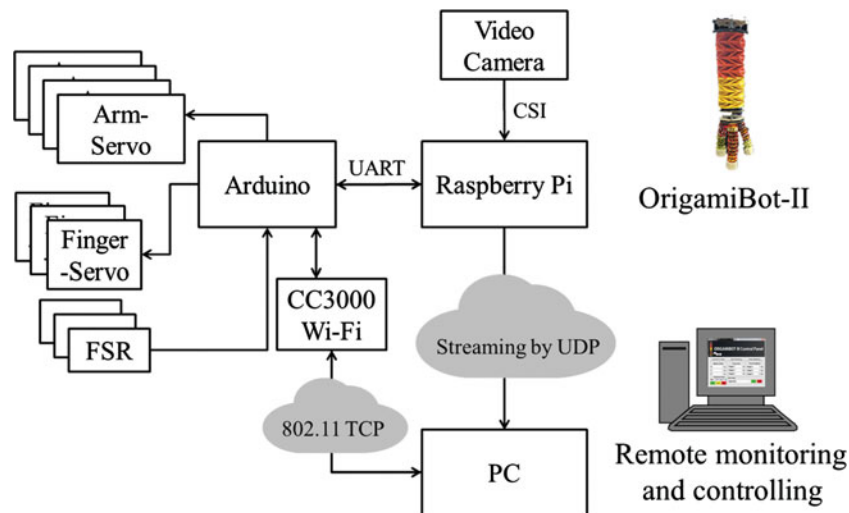


Fig. 8. Overall system architecture for internet-based control of OrigamiBot-II.

or a joystick) that are wirelessly communicating with each other. Figure 8 shows the overall system architecture. In general, communication between two computers uses a Transmission Control Protocol/Internet Protocol (TCP/IP) socket or the User Datagram Protocol (UDP). The connection between the origami manipulator and a remote control device utilizes Raspberry Pi as a main processor to send collected H264 encoded video using real-time protocol (RTP) over UDP. HTTP-based image streaming have been attempt, but the CPU usage was up around 70% and the transferred image did not scale as well as H264. Video streaming using real-time streaming protocol (RTSP) had been used over TCP but the streaming video was very slow.

A 5-megapixel video camera captures each frame (15 fps) and sends them to the Raspberry Pi using the CSI interface allowing fast and reliable high-resolution data transfer (1080 p). While streaming the video by UDP to the remote PC, the Raspberry Pi also communicates with the Arduino using a universal asynchronous receiver/transmitter (UART) to allow motor control and force feedback. Direct control from client (remote PC) is enabled via 802.11 (i.e., Wi-Fi) over TCP. A remote PC accesses to the IP address and command packet to control the servo motors and receives the force feedback. A CC3000 Wi-Fi module, attached to the Arduino, interfaces with the remote PC. On the Arduino's side, "node.js"-based script has been programmed, which is an open-source, cross-platform runtime environment for server-side networking applications written in JavaScript. A graphical user interface (GUI) written in Visual C# provides real-time video streaming, motion script generation, force limit set-up and feedback, and motion running based on script file.

#### 4.2. Manipulation capabilities

For preliminary testing of the robot's manipulation capabilities, three different objects with different shapes and weights were selected, including a shuttlecock (0.011 lb), an egg shell (0.011 lb), and a cube block with varying weight (0.02 lb–0.17 lb), as shown in Fig. 9 (top). To increase friction for better grasping, each fingertip was covered by a 3D printed cover made of flexible polyester. In future experiments, the fingers may be covered with different fingertips using different materials and shapes. OrigamiBot-II was programmed to follow four steps: (1) ready to grasp, (2) grasp the object, (3) lift the object up and bend the arm while holding the object, and (4) release the object. The entire sequence took about 10 seconds.

For an egg shell, three different initial orientations, i.e., upward (pointed end up), downward, and laying on a side, were tested. A small ring was used to place an egg in a certain orientation. Figure 9 shows snapshots from the video images captured during experiments. OrigamiBot-II showed about a 92% success rate among 100 trials for an egg oriented upward. The success rates when the egg shell was downward and laying on a side were 80% and 68%, respectively. For a shuttlecock with the base upward, OrigamiBot-II showed 42% success rate among 100 trails. The low success rate



Fig. 9. Video-captured images showing physical demonstrations of the robot's manipulation capability for five different objects.

can be attributed to the fact that the geometry of the fingers prevents them from grasping very small objects, and the diameter of the base of the shuttlecock was very near this size threshold. Due to the size, geometric shape, and smooth surface of the paper cup, the gripper could lift it only by placing one finger inside and two fingers outside of the cup (Fig. 9). Even with this strategy, it showed only

Table I. Deflection angle ( $\gamma$ ) per loaded weight.<sup>1</sup>

Weight (lb)	1	1.5	2	2.5	3
$\gamma$ (rad)	0.0524	0.1047	0.1386	0.2094	N/A

Table II. Object manipulation capability measured by the ratio of successful grasping and lifting manipulations among 100 trials for an egg shell in three different orientations, a shuttle cock, and a paper cup, and 20 trails for a cube block in five different weights.

	Object specification		
	Weight (lb)	Orientation	Success rate (%)
Egg shell	0.011	Upward	92
	0.011	Downward	80
	0.011	Side	68
Shuttlecock	0.011	Upward	42
Paper cup	0.018	Upward	8
Cube block	0.020	N/A	100
	0.080	N/A	80
	0.100	N/A	90
	0.125	N/A	55
	0.150	N/A	20
	0.170	N/A	0

8% success rate after all. This is mainly due to the current fingertip design, which does not support manipulating thin or small objects. The cube block ( $2 \times 2 \times 2 \text{ in}^3$ ) was filled with weights ranging from 0.02 to 0.17 lb, and 20 manipulation trials were performed for each weight. Until 0.1 lb, the manipulator maintained a relatively high success rate, but it begins to show poor performance with a cube weight of 0.125 lb or heavier.

For load testing, we examined the amount of load that the twisted tower could hold without damaging the structure.<sup>1</sup> In this test, 1.0, 1.5, 2.0, 2.5, and 3.0 lb of load were attached at the bottom of the arm and the deflection angle ( $\gamma$ ), relative to the maximum unloaded bending angle, was measured. As shown in Table I, the arm could bear up to 2.5 while gradual increase in  $\gamma$  was observed as the load weight increases. The amount of load that can be manipulated by OrigamiBot-II is much smaller than the results shown in Table I because it is limited by the amount of load that the fingers can grasp and hold. As shown in Table II, the maximum amount of load may also vary depending on the geometry and material on the surface. For a cube block whose surface is covered with a mat board, the maximum load for OrigamiBot-II was 0.1 lb, with a success rate of over 90%. If the origami gripper is replaced by another gripper with a better grasping performance, the arm of OrigamiBot-II can bear up to 2.5 lb with a relatively small deflection in the arm, even at its maximum bending angle. The arm was not able to lift a weight of 3 lb.

#### 4.3. Comparison with a rigid gripper

Another experiment was performed to analyze the exerted force from the gripper to the object at the points of contact. For comparison, a three-finger gripper made of rigid plastic parts with a comparable physical size was built. This rigid gripper also used a cable-actuated mechanism with the same mini servos as the origami gripper. Force Sensitive Resistors (FSRs) were attached at the fingertips of OrigamiBot-II and the rigid gripper to measure the consumed current, which is correlated to the actuator torque. To adjust the backward tension in the rigid gripper, which has a free joint at each finger, a rubber material was used. While load cells may be a better option for precise force measurement, FSRs were selected for their light weight. The relationship between force and resistance is provided by the manufacturer, while additional calibration was performed in our laboratory.

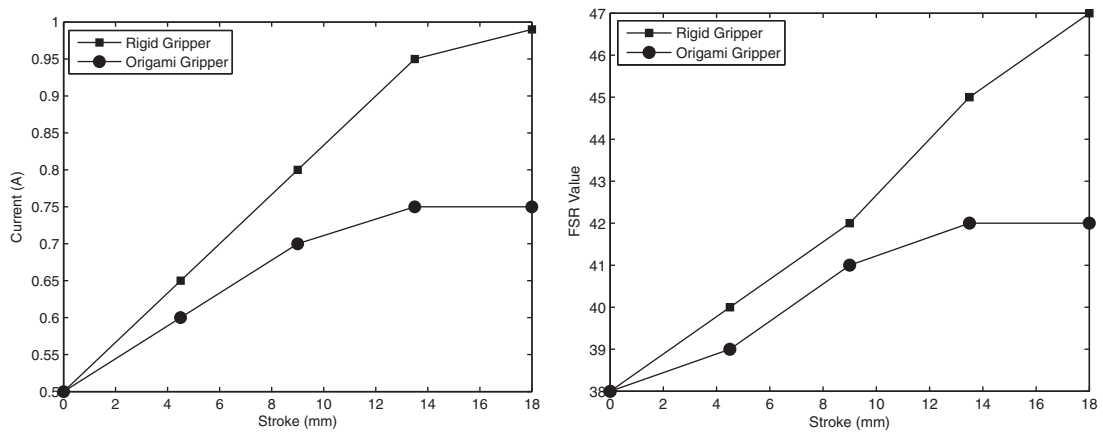


Fig. 10. Current consumption versus stroke (left) and FSR value vs. stroke (right).

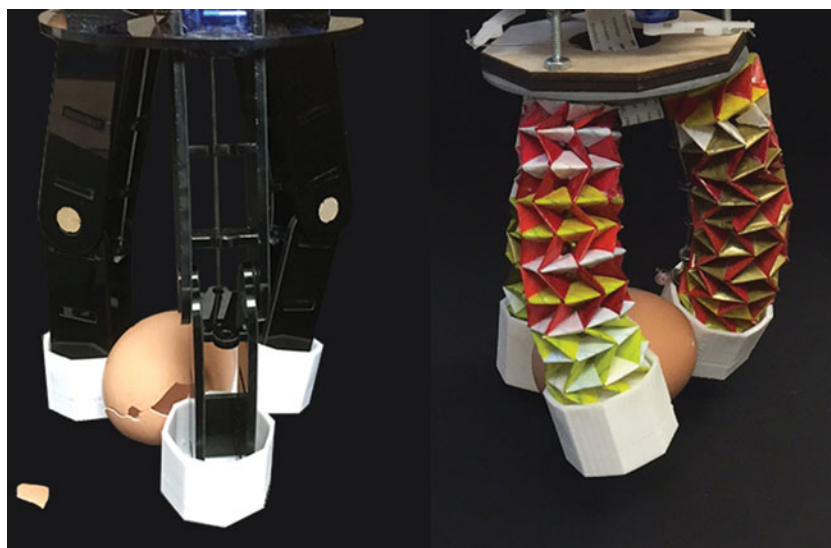


Fig. 11. The rigid gripper broke the egg shell at around 18 mm (0.7 in) stroke of pulling cable, while the origami gripper in OrigamiBot-II was able to deform the fingers wrapping around the egg shell without causing any damage.

An egg shell was used for testing exerted forces from the fingertips of the rigid gripper and the origami gripper. When the pulling force increased, the forces at the fingertips of the rigid gripper showed linear increase, while the forces at the origami fingers tended to converge to a certain threshold (Fig. 10). After the origami fingers reached this threshold, deformation was observed in its structure that makes the fingers wrap around the egg shell. Figure 11 shows an experiment performed simultaneously for an egg shell using the rigid gripper and OrigamiBot-II. The three mini servos were programmed to continuously pull the cables until they reached the maximum stroke. When the stroke exceeded around 0.7 in, the egg held by the rigid gripper broke, while that in OrigamiBot-II was remained intact. The same results were observed in three repeated tests.

## 5. Conclusion and Discussion

### 5.1. Conclusion

This paper presented the design, construction, and preliminary evaluation of the cable-actuated origami manipulator, OrigamiBot-II. Building on preliminary investigation of the twisted tower design for potential robotics applications,<sup>1</sup> the contributions of this paper are in (1) the physical construction of a novel functional manipulator where both the arm and fingers use the same origami designs in different sizes, (2) kinematics and workspace analysis; and (3) exploratory experimental results demon-

Table III. Construction cost excluding labor.

Parts	Description	Cost
Papers for arm	0.012 inch thickness paper	\$2.00
Plastic sheet for fingers	Polyethylene terephthalate	\$8.00
Raspberry Pi B+	700 MHz SoC with GPU, GPIO, display	\$29.90
Camera module	CSI interface 5 megapixel pi camera	\$24.90
SG5010	Servo motors for arm (4ea)	\$3.90 × 4
SG90	Servo motors for gripper (3ea)	\$1.20 × 4
Arduino Uno R3	16 MHz microcontroller	\$24.95
Ethernet module	W5100 chipset-based module	\$6.90
Frame for workspace	quarter inch plywood and acrylic sheets	\$10.00
Cables	Ethernet cable, USB cable	\$2.00
Power	2A adapter	\$5.90
Total		\$134.95

strating potential applications of this robot. In particular, experimental results showed the potential use of OrigamiBot-II for manipulation of fragile and/or irregularly shaped objects, which is still one of the most challenging engineering problems. In addition to potential engineering benefits, OrigamiBot-II can be built with a relatively small cost. The total cost for constructing OrigamiBot-II was \$134.95 (detailed information is provided in Table III) making it suitable for an educational and research platform.

### 5.2. Limitations

Despite the potential physically demonstrated by OrigamiBot-II, the construction papers and plastic materials used for the arm and fingers are relatively fragile and susceptible to fatigue caused by repeated folding and unfolding at creases. While the current robot runs reliably without any noticeable fracture, several structural problems in the mechanical design were identified during repeated experiments, including (1) pulleys for the cables in the arm directly attached to the servo motor without any structural support to keep the pulleys vertical; (2) cables for the fingers directly connected to the mini servos causing uneven friction and stress in the cables; and (3) hooks used to secure the cable in each finger is along the bending direction where direct physical contact is expected during object manipulation, interrupting the proper grasping of the object of the fingers and creating multiple points of contact.

Manufacturability also limits the potential use of such a novel mechanism. An origami design often involves a complex sequence of folding and bending. Some designs may also involve assembling multiple origami segments. This process is labor intensive and time consuming when performed by human hands. In addition, automation of such a process is not an easy engineering problem to solve. The existing origami folding robots can only perform “simple” folds, such as valley and mountain folds.<sup>23</sup> Nevertheless, this system implies that the folding process can be at least partially automated.

### 5.3. Discussion and future work

As illustrated in this paper, origami has great potential in addressing several design challenges in robotics, because it takes advantages of space creation (from 2D to 3D) and coexisting structural properties of flexibility and rigidity. However, little to no effort has been made to establish a theoretical framework for systematic selection of an origami design and its translation into a functional robot. Such selection and translation requires considerations from multidimensional perspectives, which may include materials, geometry, mathematical modeling, novel actuation design, and control strategies. We are still at an early stage in this long journey, beginning with physical demonstrations and implementations of origami designs to build fully functioning robots.

To address a particular challenge of manufacturability, we are currently investigating 3D printable origami designs, including the twisted tower. While further investigation is needed to identify appropriate materials to be used for the “rigid” surface and “flexible” hinges, we have printed a nearly identical structure, with the same twisting and bending motions, as a single 3D object. This early-stage work will be a pathway toward 3D printable origami structures while structural and geometrical properties are preserved.

### Acknowledgments

This work was sponsored by the Nord Distinguished Assistant Professorship. The authors would also like to thank Tao Liu, Alejandro Owen Aquino, Ishaan P. Rao, Qian Wang, and Yanzhou Wang for their assistance with experiments.

### References

1. E. Vanderhoff, D. Jeong and K. Lee, "OrigamiBot-I: A Thread-Actuated Origami Robot for Manipulation and Locomotion," *Proceedings of the IEEE/RSJ International Conference on Intelligent Robots and Systems*, pp. 1421–1426, Chicago, IL, USA, Sep. 14–18, 2014.
2. T. Tachi, "3D Origami Design based on Tucking Molecule," *Proceedings of the 4<sup>th</sup> International Conference on Origami in Science, Mathematics, and Education*, pp. 259–272, Pasadena, CA, Sep. 8–10, 2006.
3. W. Wu and Z. You, "Modeling rigid origami with quaternions and dual quaternions," *Proceedings of the Royal Society A: Mathematical, Physical and Engineering Science*, 466, 2155–2174, 2010.
4. E. Hawkes, B. An, N. M. Tanaka, S. Kim, E. D. Demaine, D. Rus, and R. J. Wood, "Programmable matter by folding," *Proceedings of the National Academy of Science of the United States of America*, **107**(28), 12441–12445 (2010).
5. P. Jackson, "Folding Techniques for Designers: From Sheet to Form," *Pap/Cdr. Laurence King Publishers* (2011).
6. M. Schenk and S. D. Guest, "Origami Folding: A Structural Engineering Approach," *Proceedings of the 5<sup>th</sup> International Meeting of Origami Science, Mathematics, and Education*, pp. 291–304, CRC Press, Boca Raton, FL, 2011.
7. N. De. Temmerman, M. Mollaert, T. Van Mele and L. De Laet, "Design and analysis of a foldable mobile shelter system," *Int. J. Space Struct.* **22**(3), 161–168 (2007).
8. J. Ma and Z. You, "The Origami Crash Box," *Proceedings of the 5<sup>th</sup> International Meeting of Origami Science, Mathematics, and Education*, pp. 277–290, CRC Press, Boca Raton, FL, 2011.
9. H. Okuzaki, T. Saido, H. Suzuki, Y. Hara, and H. Yan, "A Biomorphic Origami Actuator Fabricated by Folding a Conducting Paper," *Journal of Physics: Conference Series*, **127**(1): p. 012001, IOP Publishing, 2008.
10. R. V. Martinez, C. R. Fish, X. Chen, and G. M. Whitesides, "Elastomeric origami: Programmable paper-elastomer composites as pneumatic actuators," *Advanced Functional Materials*, **22**(7): 1376–1384 (2012).
11. C. C. Min and H. Suzuki, "Geometrical Properties of Paper Spring," *Manufacturing Systems and Technologies for New Frontier*, pp. 159–162 (2008).
12. C. D. Onal, R. J. Wood and D. Rus, "Towards Printable Robotics: Origami-Inspired Planar Fabrication of Three-Dimensional Mechanisms," *Proceedings of the IEEE International Conference on Robotics and Automation*, pp. 4608–4612, Shanghai, China, May 9–13, (2011) pp. 4608–4613.
13. D. Y. Lee, G. P. Jung, M. K. Sin, S. H. Ahn, and K. J. Cho, "Deformable Wheel Robot Based on Origami Structure," *Proceedings of the IEEE ICRA*
14. D. Jeong and K. Lee, "An Amphibious Robot with Reconfigurable Origami Wheels for Locomotion in Dynamic Environment," *Proceedings of International Mechanical Engineering Congress & Exposition*, Houston, TX, Nov. 13–19, 2015.
15. J. Koh and K. Cho, "Omegabot: Biomimetic Inchworm Robot Using SMA Coil Actuator and Smart Composite Microstructures (SCM)," *Proceedings of the IEEE International Conference on Robotics and Biomimetics*, pp. 1154–1158, Guilin, China, Dec. 18–22, 2009.
16. M. Calisti, M. Giorelli, G. Levy, B. Mazzolai, B. Hochner, C. Laschi and P. Dario, "An octopus-bioinspired solution to movement and manipulation for soft robots," *Bioinsp. Biomim.* **6**(3): 036002 (2011).
17. M. Cianchetti, M. Follador, B. Mazzolai, P. Dario and C. Laschi, "Design and Development of a Soft Robotic Octopus Arm Exploiting Embodied Intelligence," *Proceedings of the IEEE International Conference on Robotics and Automation*, pp. 5271–5276, Saint Paul, Minnesota, USA, May 14–18, 2012.
18. C. Li and C. D. Rahn, "Design of continuous backbone and cable driven robots," *Journal of Mechanical Design*, **124**(2): 265–271 (2002).
19. M. Hannan and I. D. Walker, "Kinematics and the implementation of an elephant's trunk manipulator and other continuum style robots," *Journal of Field Robotics*, **20**(2): 45–63.
20. W. McMahan, M. Pritts, V. Chitrakara, D. Dienno, B. Jones, M. Grissom, M. Csencsits, V. Iyengar, I. D. Walker, C. D. Rahn and D. Dawson, "Design and Experimental Testing of the OctArm Soft Robot Manipulator," *SPIE Defense and Security Symposium*, Orlando, FL, April 18–20, 2006.
21. S. Felton, M. Tolley, E. Demaine, D. Rus, and R. Wood, "A method for building self-folding machines," *Science* **345**(6197), 644–646 (2014).
22. N. G. Cheng, M. B. Lobovsky, S. J. Keating, A. M. Setapen, K. I. Gero, A. E. Hosoi, and K. D. Iagemma, "Design and Analysis of a Robust, Low-Cost, Highly Articulated Manipulator Enabled by Jamming of Granular Media," *Proceedings of the IEEE International Conference on Robotics and Automation*, Saint Paul, Minnesota, USA, May 14–18, 2012.
23. D. J. Balkcom and M. T. Mason, "Robotic origami folding," *International Journal of Robotics Research*, **27**(5): 613–627 (2008).